

## Unpredicted porosity improvement upon thermal reactivation of a fouled multi-walled carbon nanotube

Zarubina, Valeriya; Mercadal, Juan J.; Jansma, Harrie; Melián-Cabrera, Ignacio

**DOI**

[10.1016/j.matlet.2024.136386](https://doi.org/10.1016/j.matlet.2024.136386)

**Publication date**

2024

**Document Version**

Final published version

**Published in**

Materials Letters

**Citation (APA)**

Zarubina, V., Mercadal, J. J., Jansma, H., & Melián-Cabrera, I. (2024). Unpredicted porosity improvement upon thermal reactivation of a fouled multi-walled carbon nanotube. *Materials Letters*, 364, Article 136386. <https://doi.org/10.1016/j.matlet.2024.136386>

**Important note**

To cite this publication, please use the final published version (if applicable). Please check the document version above.

**Copyright**

Other than for strictly personal use, it is not permitted to download, forward or distribute the text or part of it, without the consent of the author(s) and/or copyright holder(s), unless the work is under an open content license such as Creative Commons.

**Takedown policy**

Please contact us and provide details if you believe this document breaches copyrights. We will remove access to the work immediately and investigate your claim.



# Unpredicted porosity improvement upon thermal reactivation of a fouled multi-walled carbon nanotube

Valeriya Zarubina<sup>a,b</sup>, Juan J. Mercadal<sup>b</sup>, Harrie Jansma<sup>c</sup>, Ignacio Melián-Cabrera<sup>b,d,\*</sup>

<sup>a</sup> Erasmus University College (EUC), Erasmus University Rotterdam, Nieuwemarkt 1A, 3011 HP Rotterdam, The Netherlands

<sup>b</sup> Faculty of Science and Engineering, University of Groningen, Nijenborgh 4, 9747 AG Groningen, The Netherlands

<sup>c</sup> Catalysis Engineering, Department of Chemical Engineering, Faculty of Applied Sciences, Delft University of Technology, Van der Maasweg 9, 2629 HZ Delft, The Netherlands

<sup>d</sup> Applied Photochemistry and Materials for Energy Group, University of La Laguna, Avda. Astrofísico Francisco Sánchez, s/n, PO Box 456, 38200 San Cristóbal de La Laguna, S/C de Tenerife, Spain

## A B S T R A C T

Deposition of carbonaceous species on a solid catalyst's surface during a catalysed processes is quite usual. This causes fouling, or depletion of the textural features, with a performance decay. In this work, preliminary results for an *ex situ* thermal oxidative reactivation of a fouled MWCNT are presented. The coke is nearly completely removed and, as a side effect, some of the MWCNT is combusted. Remarkably, the textural features are improved; 23 % higher BET area and 29 % higher total pore volume, while maintaining the isotherm shape. These improvements are attributed to two factors. Firstly, the removal during reactivation of non-porous (or less-porous) carbon domains present in the starting MWCNT, that positively influences the porosity in various ways; a control experiment employing the fresh MWCNT strongly suggests this hypothesis. Secondly, the new microporosity also contributes to the better BET.

## 1. Introduction

A central concern these days is the availability of critical elements [1], and their impact on industrial technologies, e.g. catalytic technologies [2]. In this context, carbon-based materials can play a significant role due to the high element abundance. Multiwalled carbon nanotubes (MWCNTs) is a group of materials that have attracted wide industrial and academic interest, e.g. as high-performance microwave absorbing materials [3,4]. MWCNTs have been claimed active in a chemical reaction of industrial interest: the oxidative dehydrogenation of ethylbenzene into styrene (EB-ODH reaction) [5,6].

This reaction produces coke (ODH-coke), which is also active for the reaction [7,8]. Though the MWCNT is initially active and selective, the deposited coke dominates the performance [6,9]. This typically happens under industrially-relevant reaction conditions, as proven on various catalyst types [6,8–12]. The main deactivation here is the over-coking, i. e., the continued coke deposition which decreases the surface area and pore volume [6,8,9,12]. Eventually the catalyst bed would be plugged, leading to run-away/explosive conditions. Therefore, removal of the excessively-deposited ODH-coke needs to be done to continue the operation. This can be done thermally with an oxidant (e.g. O<sub>2</sub>/N<sub>2</sub> mixture or air) for thermally-stable inorganic-based catalysts [8,11,13]. It is however challenging for MWCNTs and generally for any carbon-

based material. This is because the MWCNT would undergo combustion/gasification during the oxidative thermal removal of the ODH-coke.

In this work, we report preliminary results for the ODH-coke removal using an *ex situ* method that maximizes heat and O<sub>2</sub>-transfer across the material.

## 2. Experimental methods

### 2.1. Materials

The MWCNT was provided by Hyperion (CS-02C-063-XD). A 212–425 μm fraction was used for the catalytic test, reactivation and characterization.

### 2.2. Reactivation

The reactivation was carried out in a Nabertherm RT 50/250–11 tubular oven. The sample was loaded in a quartz crucible and placed at the furnace's isothermal heating zone. After purging, the temperature was raised from room temperature to 450 °C, at 3 °C/min and held for 2, 5 or 24 h, in a 1 % vol. O<sub>2</sub>/Ar flow stream (150 mL/min STP).

\* Corresponding author.

E-mail address: [ignacio.melian.cabrera@ull.edu.es](mailto:ignacio.melian.cabrera@ull.edu.es) (I. Melián-Cabrera).

<https://doi.org/10.1016/j.matlet.2024.136386>

Received 3 February 2024; Received in revised form 11 March 2024; Accepted 26 March 2024

Available online 27 March 2024

0167-577X/© 2024 Elsevier B.V. All rights reserved.

### 2.3. Characterization

The procedures for thermogravimetric analysis (TGA), TPO and N<sub>2</sub> physisorption can be found elsewhere [14–16].

### 3. Results and discussion

The fouled MWCNT was obtained following the catalytic test reported previously [6]. Thermogravimetric analysis (Fig. 1A) shows a shift towards lower temperatures of the MW-S (fouled material). This is due to new deposited species, the ODH-coke. The effect can be better seen in Fig. 1B (TPO) with two distinctive steps. The lower-temperature peak is due to the ODH-coke's combustion whereas the higher-temperature one corresponds to the MWCNT's combustion. For simplicity, we refer these as combustion processes but gasification can also take place simultaneously. The intensity of the ODH-coke's TPO peak (Fig. 1B) is used to assess the coke removal.

The porosity of the fouled material shows decreased BET area and pore volume (Table S1), in line with the deposition of ODH-coke observed by TGA/TPO.

The reactivation procedure is sketched in Fig. 1C. Reactivation refers in this study to the process of ODH-coke removal rather than to the catalytic properties, which fall outside the scope of this work. The first step corresponds to the deposition of ODH-coke by the reaction (weight increase), whereas the second one is the coke's combustion during reactivation (weight decrease). The choice of 450 °C is based on the TPO patterns (Fig. 1B) where the combustion rate of the ODH-coke is higher than that of the MWCNT (ca. four times higher). Some combustion of the MWCNT is however expected. Temperature may be further optimised to shorten the processing time.

The TPOs of the reactivated materials upon various treatment times are shown in Fig. 2. Clearly, the ODH-coke is removed over time. The final case, treated for 24 h, does not show the ODH-coke peak. This outcome is positive because it shows that ODH-coke can be fully removed by an oxidative thermal treatment, while the MWCNT remains.

The porosity was assessed by N<sub>2</sub> physisorption, Fig. 3. The MW-Fr displays an isotherm type IV with H1 hysteresis [17] and a bimodal pore size distribution. Some type II character is also present as the isotherm does not level off at  $P/P_0$  near 1 [17,18]. The isotherm for the fouled MW-S, with the same shape, displays much lowered adsorption values, associated to the deposition of ODH-coke. The reactivated

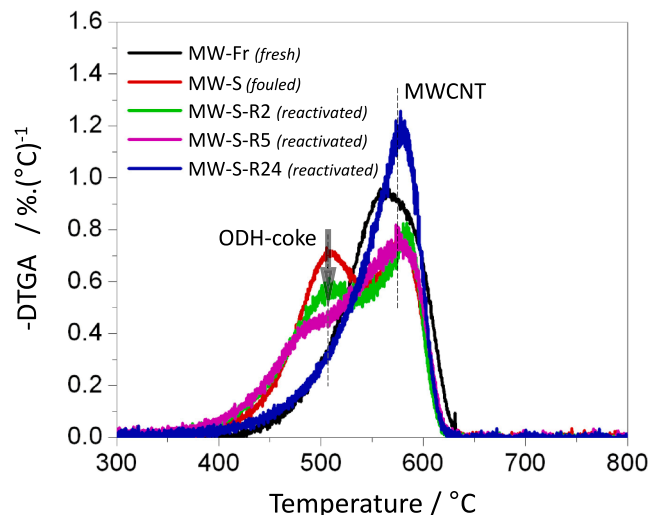


Fig. 2. TPO patterns of the MWCNT materials upon reactivation (MW-S-R2, -R5 and -R24), fresh (MW-Fr) and fouled (MW-S) materials.

materials, also displaying the same shape, gradually shift upwards regaining the adsorption capacity (Fig. 3A). This is also seen in the BJH pore size distribution (Fig. 3B); both the main and secondary pores increase in intensity with the treatment time. Even, the 24 h-treated material surpasses the fresh counterpart, both the isotherm and the pore size distribution. These interesting observations will be discussed later.

The textural parameters are represented in Fig. 4. The new microporosity in the reactivated materials is ascribed to micropores formed in the ODH-coke by gasification/combustion, during the reactivation. It is not expected that such microporosity occurs in the MWCNT in view of its higher oxidation stability as compared to more amorphous carbons (i.e., ODH-coke) [19]. The microporosity drops for the final material, MW-S-R24. The small microporosity in this material is attributed to residual porous ODH-coke, which is likely invisible in the TPO due to the broad shoulder (Fig. 2).

Surprising findings are the enhanced BET area and total pore volume for MW-S-R24, higher than those of the starting MWCNT (MW-Fr), with 23 % and 29 % increase respectively while preserving the isotherm shape. The increase in BET area cannot only be ascribed to the new micropores (Fig. 4A), since the difference between MW-S-R24 and MW-Fr ( $\Delta S_{\text{BET}} = 95 \text{ m}^2/\text{g}$ ) is larger than the new microporosity in MW-S-R24 ( $S_{\text{micro}} = 30 \text{ m}^2/\text{g}$ ;  $\sim 1/3$  of the difference). The same happens to the total pore volume, that cannot be explained by the microporosity. These effects can be tentatively explained by the removal, by combustion during reactivation, of non-porous domains present in the native MW-Fr. It is normal that different types of carbon allotropes, including non-porous amorphous domains, coexist in a commercial material [14,20,21] as the one employed here. The removal of such non-porous species can take place during the reactivation by selective combustion since its reactivity towards O<sub>2</sub> is higher than the MWCNT. This is supported by evidence proving that amorphous carbon oxidizes faster than the carbon nanotube [19]. In other words, a high density of defects in amorphous carbon makes it relatively easy to eliminate by oxidation [20]. The higher total pore volume for MW-S-R24 than the fresh MWCNT (Fig. 4B) is due to larger mesopores being formed; see new peak centered at ca. 45 nm and the broad shoulder towards higher values (Fig. 3B). The internal pore remains unchanged (ca. 3 nm). The larger pore size is attributed to the removal by combustion/gasification of non-porous carbon domains/particles located between the tubes in the fresh MWCNT. The higher BET area can also be explained (partly) by the removal of non-porous carbon, where one gram of material would contain more porous material and hence a higher BET area is expected. This aspect also positively affects the total pore volume. This type of

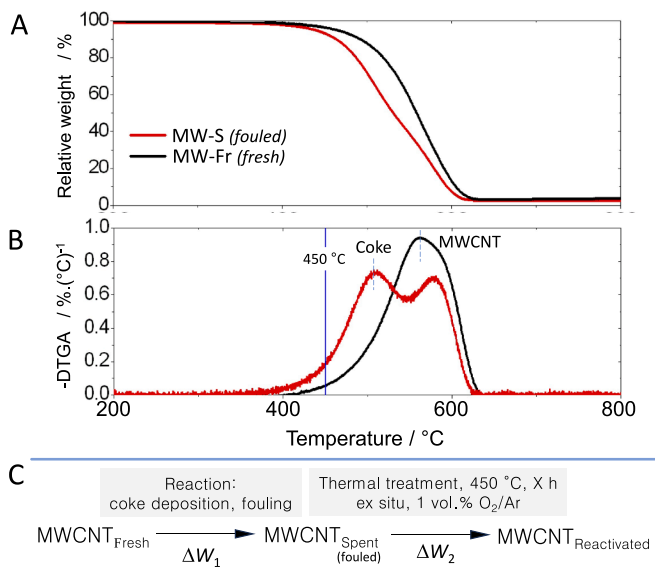
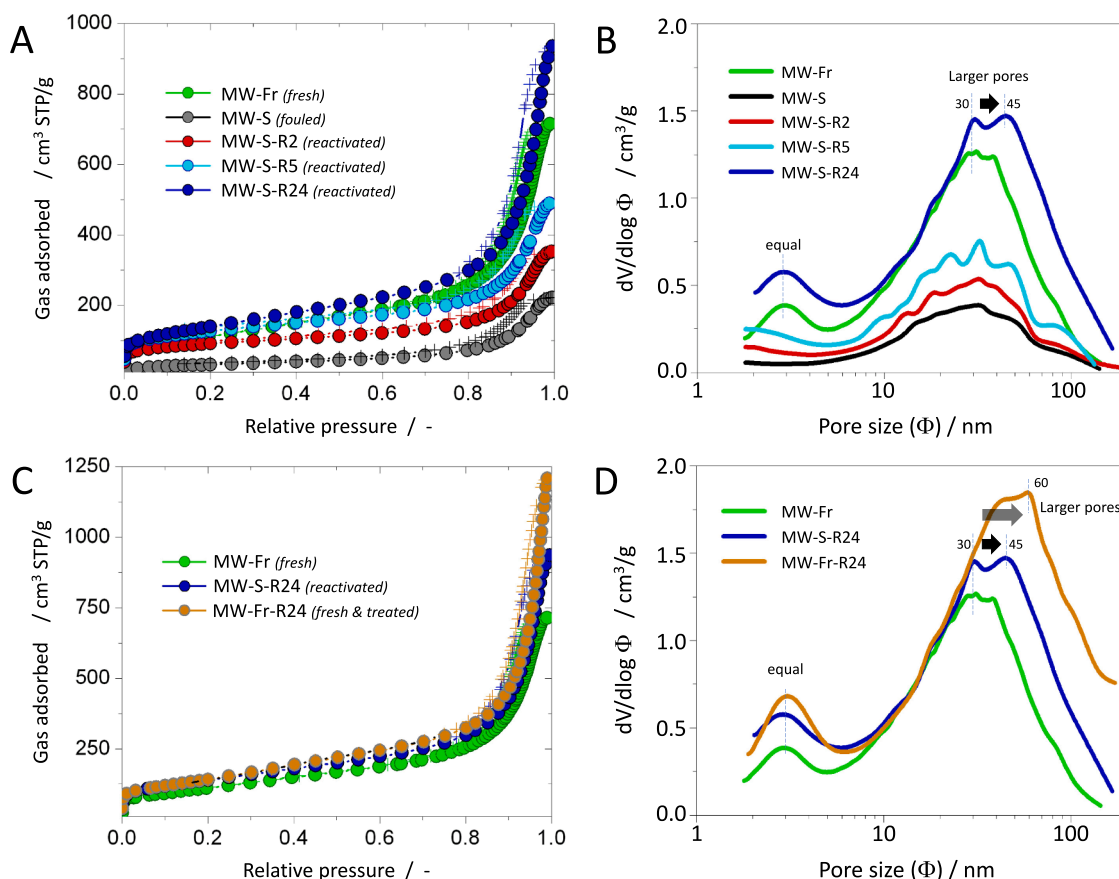
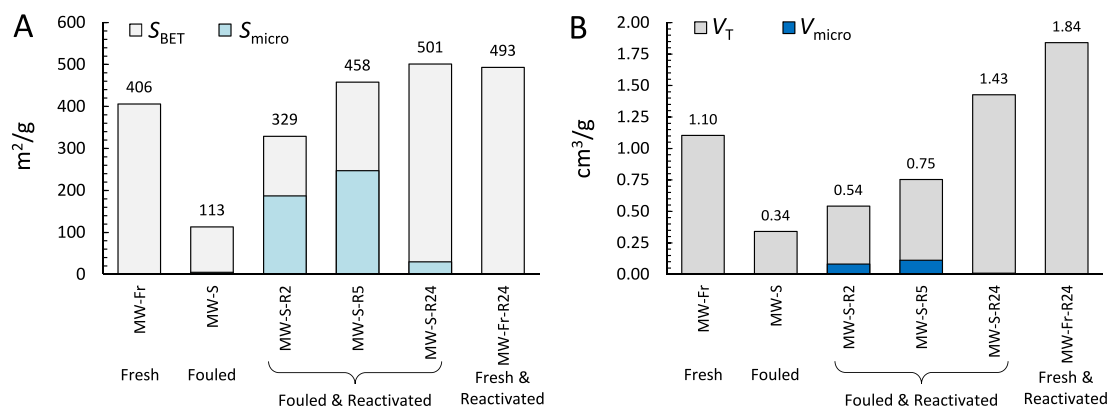


Fig. 1. A) Thermogravimetric analysis in air of the fresh (MW-Fr) and fouled MWCNT (MW-S). B) TPO patterns given as -DTGA (derivative of the TGA curve). C) Experimental plan for the reactivation.



**Fig. 3.** A)  $N_2$  physisorption isotherms for MWCNT materials after reactivation (MW-S-R2, -R5 and -R24), fresh (MW-Fr) and fouled (MW-S) materials. B) BJH pore size distributions derived from  $N_2$  physisorption data for materials described in A. C)  $N_2$  physisorption isotherm for MW-Fr-R24 (this material was obtained by treating the fresh MWCNT following the same reactivation procedure for 24 h); the graph also includes the fresh MW-Fr and reactivated MW-S-R24 for comparison. D) BJH pore size distributions derived from  $N_2$  physisorption data for the materials described in C. In B and D, the adsorption branch was employed for relative comparative purposes; the desorption data gave significant scattering.



**Fig. 4.** Surface areas,  $S_{BET}$  and  $S_{micro}$  (A) and pore volumes,  $V_T$  and  $V_{micro}$  (B). The microporosity columns are not stacked but overlaps the  $S_{BET}$  and  $V_T$ , to highlight the contribution of the microporosity to the total values. Raw data can be found in Table S1.

carbon might also be less-porous than the MWCNT, rather than non-porous, and the same explanation holds. Moreover, the residual microporosity contributes in ca. 1/3 of the BET's improvement but not much in the total pore volume's increase.

A control experiment was carried out for additional evidence. The fresh MWCNT was treated following the same reactivation procedure as for MW-S-R24, denoted as MW-Fr-R24. The textural parameters were notably improved whilst maintaining the same isotherm shape (Fig. 3C,

Fig. 4A, and Fig. 4B); 21 % for  $S_{BET}$  and 67 % for  $V_T$ . The BET area was comparable to the reactivated MW-S-R24, whereas the total pore volume increased even further. Such a high total pore volume is due to larger mesopores formed (60 nm and beyond, Fig. 3D). The internal pore remains unchanged (ca. 3 nm). No microporosity was detected, which supports the above discussion; the residual microporosity in the reactivated materials should be located in the residual ODH-coke. Both improvements here,  $S_{BET}$  and  $V_T$ , are ascribed to the removal of non-

porous/less-porous domains present in the MWCNT by gasification/combustion; this makes the mesopores larger (higher  $V_T$ ) and, moreover, there is more porous material per gram (higher  $S_{BET}$  and  $V_T$ ). There is no microporosity contribution nor smaller mesopores, that often contribute to higher BET areas [13,15,22,23]; actually, it has larger mesopores. Therefore, the enhanced BET must only come from the removal of non-porous/less-porous domains resulting in more porous material per mass. These results strongly support the previous interpretation of the removal of non-porous/less-porous domains in the starting MWCNT during the reactivation of the fouled material, leading to enhanced textural parameters.

A final aspect is the mass efficiency of the process, of the consecutive reactions taking place on the MWCNT:



where,

$$\Delta W_1 = \frac{W_S - W_F}{W_F} \quad (2)$$

$$\Delta W_2 = \frac{W_R - W_S}{W_S} \quad (3)$$

$W$  is weight, and the subscripts F, S, and R mean fresh, spent (fouled) and reactivated, respectively. The overall mass difference can be calculated as:

$$\Delta W_T = \frac{W_R - W_F}{W_F} \quad (4)$$

By obtaining  $W_R$  from eqs. (2) and (3) as a function of  $W_F$ , the following relation can be obtained:

$$\Delta W_T = \Delta W_1 + \Delta W_2 + \Delta W_1 \Delta W_2 \quad (5)$$

Under the applied conditions, the following values were obtained:

$$\Delta W_1 = +0.80 \text{ and } \Delta W_2 = -0.58 \text{ (value for MW-S-R24).}$$

This yields an overall mass difference of  $\Delta W_T = -0.24$ . Therefore, 24 % of the starting MWCNT is combusted in the reactivation (24 h treatment). This is not surprising since the TPO pattern showed that the MWCNT's oxidation rate at 450 °C was not zero (Fig. 1B).

Concluding, an oxidative thermal treatment of a coke-fouled MWCNT removes the coke almost entirely. The process also combusts/gasifies some of the MWCNT. Remarkably, the reactivation notably improves the BET area and total pore volume. These improvements are interpreted by two factors. Firstly, the removal by combustion/gasification of non-porous (or less-porous) carbon domains in the starting MWCNT, leading to larger pores (higher  $V_T$ ) and more porous material per mass (higher  $S_{BET}$  and  $V_T$ ). A control experiment employing the fresh MWCNT strongly suggests this hypothesis. Secondly, the new microporosity also contributes to the improved BET ( $\sim 1/3$ ) but hardly in the pore volume.

#### CRedit authorship contribution statement

**Valeriya Zarubina:** Writing – review & editing, Investigation, Data

curation, Conceptualization. **Juan J. Mercadal:** Writing – review & editing, Investigation, Data curation. **Harrie Jansma:** Writing – review & editing, Resources, Investigation, Data curation. **Ignacio Melián-Cabrera:** Writing – original draft, Resources, Project administration, Funding acquisition, Data curation, Conceptualization.

#### Declaration of competing interest

The authors declare that they have no known competing financial interests or personal relationships that could have appeared to influence the work reported in this paper.

#### Data availability

Data will be made available on request.

#### Acknowledgements

This work was supported by the Dutch Technology Foundation STW (STW07983), a division of the Netherlands Organization for Scientific Research (NWO) and Vidi Grant 10284 (NWO). The manuscript was completed by I.M.C. (data curation, interpretation and writing) at La Laguna University. Dr. M. Makkee and Dr. C. Nederlof are thanked for their contributions in the STW project.

#### Appendix A. Supplementary data

Supplementary data to this article can be found online at <https://doi.org/10.1016/j.matlet.2024.136386>.

#### References

- [1] G.A. Blengini, et al., *Resour. Policy* 53 (2017) 12–19.
- [2] I. Melián-Cabrera, *Ind. Eng. Chem. Res.* 60 (2021) 18545–18559.
- [3] T. Jia, et al., *Carbon* 206 (2023) 364–374.
- [4] L. Kong, et al., *Int. J. Miner. Metall. Mater.* 30 (2023) 570–580.
- [5] J. Zhang, et al., *Angew. Chemie - Int. Ed.* 46 (2007) 7319–7323.
- [6] V. Zarubina, et al., *Carbon* 77 (2014) 329–340.
- [7] A.E. Lisovskii, C. Aharoni, *Catal. Rev.* 36 (1994) 25–74.
- [8] V. Zarubina, et al., *J. Mol. Catal. A Chem.* 381 (2014) 179–187.
- [9] J.J. Mercadal, et al., *Mol. Catal.* 529 (2022) 112525.
- [10] I. Melián-Cabrera, V. Zarubina, *Mol. Catal.* 524 (2022) 112301.
- [11] C. Nederlof, et al., *Appl. Catal. A Gen.* 476 (2014) 204–214.
- [12] V. Zarubina, et al., *Appl. Catal. A Gen.* 514 (2016) 173–181.
- [13] V. Zarubina, I. Melián-Cabrera, *Scr. Mater.* 194 (2021) 113679.
- [14] J.J. Mercadal, et al., *Chem. Eng. J.* 455 (2023) 140723.
- [15] I. Melián-Cabrera, et al., *Microporous Mesoporous Mater.* 366 (2024) 112940.
- [16] L.L. Pérez, et al., *Chem. Mater.* 25 (2013) 3971–3978.
- [17] M. Thommes, et al., *Pure Appl. Chem.* 87 (2015) 1051–1069.
- [18] I. Melián-Cabrera, V. Zarubina, *Microporous Mesoporous Mater.* 354 (2023) 112549.
- [19] Y.S. Park, et al., *Carbon* 39 (2001) 655–661.
- [20] P.X. Hou, et al., *Carbon* 46 (2008) 2003–2025.
- [21] J.H. Lehman, et al., *Carbon* 49 (2011) 2581–2602.
- [22] L.L. Pérez, et al., *J. Mater. Chem. A* 1 (2013) 4747–4753.
- [23] L. López-Pérez, et al., *Microporous Mesoporous Mater.* 319 (2021) 111065.